

<http://ansinet.com/itj>

ITJ

ISSN 1812-5638

INFORMATION TECHNOLOGY JOURNAL

ANSI*net*

Asian Network for Scientific Information
308 Lasani Town, Sargodha Road, Faisalabad - Pakistan

An Approach of Input Power Control in ICPT System with Uncertainty Load

¹Zhijun Jian, ²Zhihui Wang, ²Ning Zhang, ²Siqing Fu, ²Bo Liu and ²Xin Hu

¹China Oilfield Services Limited, Sanhe, 065201, Hebei, China

²College of Automation, Chongqing University, 400030, Chongqing, China

Abstract: In the voltage-fed Inductively Coupled Power Transfer (ICPT) system, input current increased when load become lighter especially no-load which led to system unstable. A method of frequency adjustment without adding additional links was presented which could realize the control of input power. The mathematical relationship between the input power and system operating frequency, load resistance, input voltage in the voltage-fed ICPT system was built based on mutual inductance theory. In order to improve the rapidity and accuracy of the control method, the neural network control strategy which included control network with three layers was added in the proposed method. Practical experiment illustrated that the method could make the system with good robustness when load changes in large scale. In instance, as the load resistance varied from 20-50 Ω , the input current returned to the reference value within a short time which verified that the proposed control approach was effective for ICPT system.

Key words: Inductively coupled power transfer (ICPT), input power control, uncertainty load, frequency regulation

INTRODUCTION

Inductively Coupled Power Transfer (ICPT) technology is developed to produce high-frequency magnetic field to deliver power wirelessly from the power source to load side by coupling (Tang *et al.*, 2009; Boys *et al.*, 2003; Hu, 2001). Nowadays, ICPT technology is already used in many situations, like wireless power supply of household electrical appliances, mobile phone wireless charging, electric vehicle wireless charging, etc. Because there is no physical connection between primary side and secondary side, system controller in the primary side can't learn the secondary loading condition. It's possible that the primary side appeared overpower situations. In order to improve system reliability and protect circuits it's necessary to control the input power in the primary side (Si *et al.*, 2008; Li *et al.*, 2012).

The input power is controlled according to load resistor demand. Load detection and wireless communication are added to ICPT system. The controller in the primary side can control the input power via load information from the secondary side. A kind of accurate load detection method is proposed to learn load information from the primary side (Wang *et al.*, 2013a). But in practical applications, load resistor is continuous variable. This method can't real-time detect. A simplified method for load detection is proposed to learn load information (Wang *et al.*, 2012). But its practical applications has disadvantage, power control is very complex in this way. The method of controlling the power is proposed to control the input power (Sun *et al.*, 2012).

But it needs communication from the secondary side to the primary side so that the controller learns the load information and it needs many sensors to obtain circuit parameters. Constant-current control in the primary side is another method to control the input power (Wu *et al.*, 2013; Tian *et al.*, 2012). But the constant-current control in this method needs to introduce another circuit and the controller is relatively more complicated. As for the problems above, the proposed method can control the input power without additional circuits through a simplified controller.

This study uses the typical SS-type voltage-fed ICPT system as an example. First, the influence factor of the system input power is analyzed. Combined with actual situation and system simplification, a simplified method based on frequency adjustment to control the input power is proposed. And the actual controller is designed. The feasibility of this method is verified by experiments. In case of the uncertainty of load, the input power is controlled without overshoot from the primary side.

ANALYSES OF SYSTEM INPUT CHARACTERISTICS

Aimed at controlling input power, factors which influence input power in the voltage-fed ICPT Systems need to be analyzed. The ICPT system can be classified by voltage-fed systems and current-fed systems. Based on the compensation style of the primary and secondary windings, voltage-fed ICPT systems can be further classified into SS and SP types. Current-fed

ICPT systems can also be further classified into PS and PP types (Wang *et al.*, 2004). The schematic diagram of SS-type voltage-fed ICPT system is shown in Fig. 1.

In the SS-type voltage-fed ICPT system, the DC voltage E_{dc} is selected as an energy source and the inversion network comprises four MOSFET switched, S_1 , S_2 , S_3 and S_4 . Two switch pairs (S_1 , S_4) and (S_2 , S_3) work in complementary mode to emerge square wave voltage output. The series resonant tank consists of an inductor L_p (transmitting coil) in series with a capacitor C_p (compensating capacitor) and a series inherent resistor R_p . The resonant network produces a high-frequency magnetic field to transmit energy. In the secondary side, the pickup network consists of an inductor L_s and a compensating capacitor C_s . The pickup winding receives energy from the high-frequency magnetic field. A rectifier converted high-frequency AC voltage into a constant DC voltage is made up of four diodes as a full-bridge rectifier. The DC voltage is supplied for load resistor R_L . R_L is variable continuously. M is the mutual inductance between L_p and L_s . R_s is a series inherent resistor in pickup winding.

Based on the analyses made before and energy transfer recurred to fundamental component in the resonant converter, the power of load resistor R_L is supplied by fundamental component of resonance voltage. Therefore, loading effect of the load resistance R_L on the secondary resonant circuit (Wang *et al.*, 2013b; Hu, 2001) is equivalent to R_{eq} and it is shown as 1:

$$R_{eq} = \frac{8}{\pi^2} R_L \quad (1)$$

The load impedance of the secondary is calculated as a lumped impedance (Z_s) whose value depends on the secondary compensation as given by:

$$Z_s = j\omega L_s + \frac{1}{j\omega C_s} + R_s + R_{eq} \quad (2)$$

The loading effect of the secondary on the primary circuit is shown in Fig. 2a as a reflected impedance (Z_r). The reflected impedance is calculated by the transformer coupling and operating frequency and is given (Wang *et al.*, 2004; Zhang *et al.*, 2013) by:

$$Z_r = \frac{\omega^2 M^2}{Z_s} \quad (3)$$

The output voltage of the inverter network in RMS u_{oc} can be calculated (Li *et al.*, 2013; Wu *et al.*, 2011) by:

$$u_{ac} = \frac{2\sqrt{2}}{\pi} E_{dc} \quad (4)$$

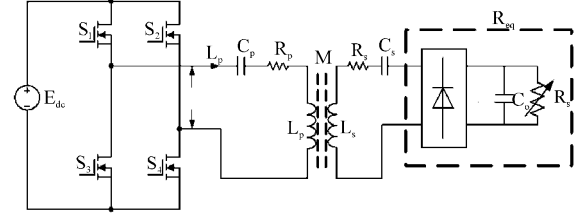


Fig. 1: Schematic diagram of SS-type voltage-fed ICPT system, E_{dc} : DC input supply, $S_1 \sim S_4$: Inverter network, Metal Oxide Semiconductor Field Effect Transistor (MOSFET), u_{ac} : Inverse voltage, (C_p , L_p): Primary resonance network, I_p : Resonance current, M : Mutual inductance, (C_s , L_s): Secondary resonance network, C_o : Filter capacitor, R_L : Load resistor, R_{eq} : Equivalent resistance, (R_p , R_s): A series inherent resistor

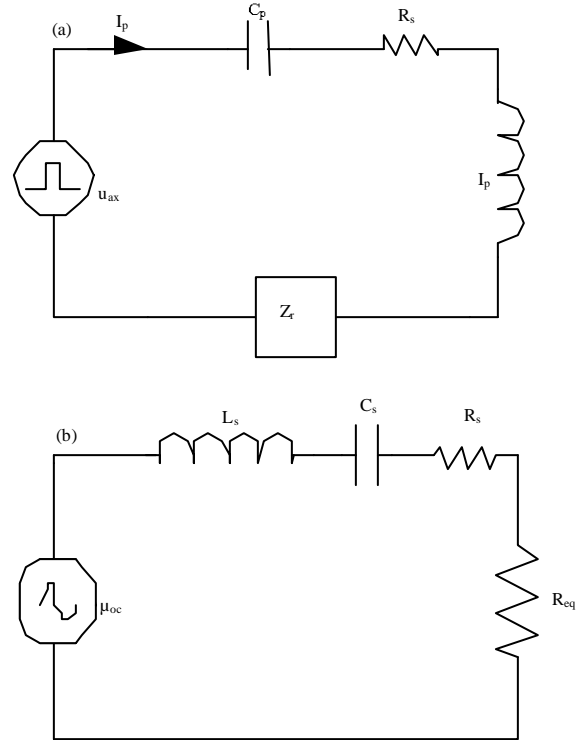


Fig. 2(a-b): Equivalent circuit diagrams of ICPT system, Z_r : Reflected impedance on the primary circuit, u_{oc} : Induced voltage in the secondary side, (a) Equivalent circuit of primary side and (b) Secondary side, loading effect of R_L on the secondary side

Then, the SS-typed voltage-fed ICPT system is simplified as shown in Fig. 2a.

If the system is operated at the resonant frequency, the primary resonance current can be calculated by:

$$I_p = \frac{u_{ac}}{Z_r} \quad (5)$$

Due to the primary series inherent resistor is small, R_p is negligible. The induced voltage in the secondary side is calculated by the primary current I_p and can be expressed as:

$$u_{oc} = \omega M I_p \quad (6)$$

The equivalent circuit of the secondary side is shown as Fig. 2b. The current in the secondary side is calculated by:

$$I_s = \frac{u_{oc}}{Z_s} \quad (7)$$

The input power consists of coil loss in the primary and secondary side with load resistance power.

$$P_{in} = I_p^2 R_p + I_s^2 R_s + I_s^2 R_L \quad (8)$$

Substituting Eq. 1-7 to 8 and Eq. 8 can be rewritten as:

$$P_{in} = \frac{E_{dc}^2}{2\pi^2 f^4 M^4} R_p + \frac{2E_{dc}^2}{\pi^4 f^2 M^2} R_s + \frac{16E_{dc}^2}{\pi^5 f^2 M^2} R_L \quad (9)$$

According to Eq. 9, the input power is related to the system operating frequency f , the input voltage E_{dc} , the mutual inductor M , load resistor R_L , the primary series inherent resistor R_p and the secondary series inherent resistor R_s . In practical applications, the mutual inductor M , the primary series inherent resistor R_p and the secondary series inherent resistor R_s are constant. E_{dc} is supplied by a certain power source. Also, E_{dc} is constant. Thus, the input power P_{in} is determined by the system operating frequency f and load resistor R_L . The relation between the input power P_{in} and the system operating frequency f with load resistor R_L is shown in Fig. 3.

When the system is operating at frequency 20 kHz, the relation between the input power and load resistance is shown in Fig. 4a. In practical applications, the high load resistance is considered to be the conditions of light load. When the system is in state of light load, the input power should be small. From Fig. 4a, the situation is just the opposite.

When the load resistor is 50 Ω , the relation between the input power and the system frequency is shown in Fig. 4b.

Based on the analyses made, when the load resistor is changed, the system frequency can be changed to

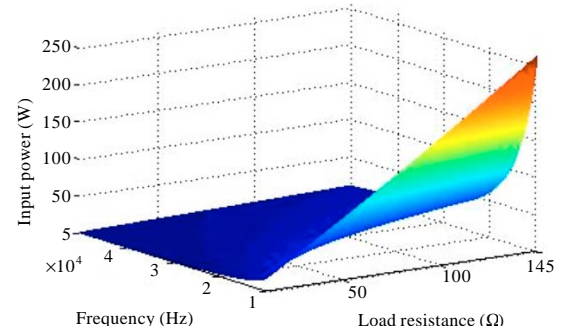


Fig. 3: Relational graph of input power with operating frequency and load resistance

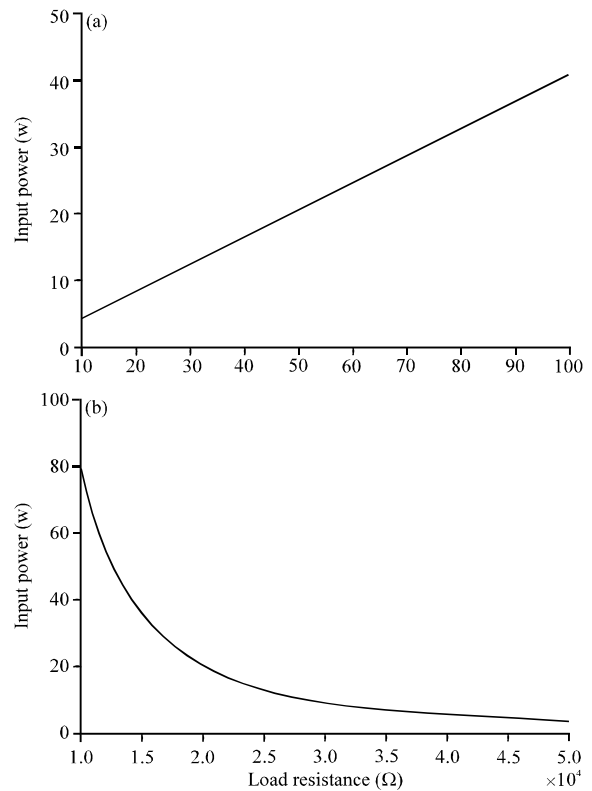


Fig. 4(a-b): Separate relational graph of input power with load resistance and frequency

control the input power. The input power can be improved via reducing the system operating frequency and reduced via rising frequency.

INPUT POWER CONTROL STRATEGY BASED ON BP NEURAL NETWORK

In order to improve the rapidity and accuracy of the control method, the neural network control strategy which included control network with three layers was added in

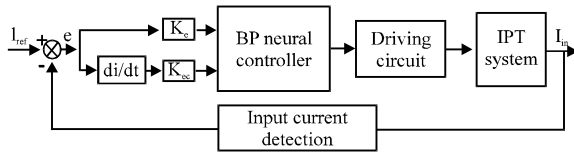


Fig. 5: Control configuration based on BP neural network

the proposed method. Based on the analyses in the previous section, the input power is changed with the system operating frequency. So the input power can be controlled by changing the system operating frequency. A control strategy based on BP neural network is proposed in this study. Its central idea is: According to input power need and setting the reference value I_{ref} of input current. Compared with the value of input power, the error and error rate of speed are regarded as the input of neural network controller. The output of controller, namely a square wave which can change period, can control the ICPT system after driving transformation. Its control configuration is shown in Fig. 5.

The ICPT system is a complex higher-order nonlinear system. It is impossible to obtain accurate model. In the modern control theory, neural network can approximate any continuous nonlinear functions, independent of its concrete model.

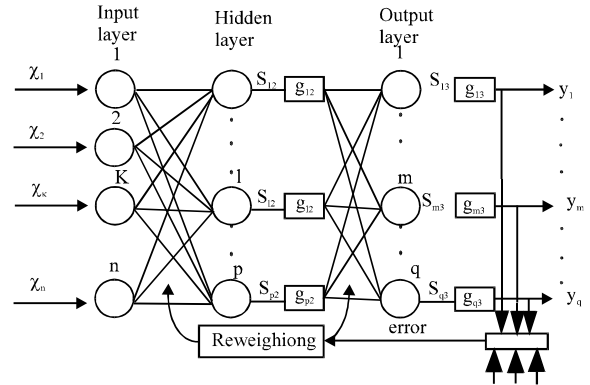
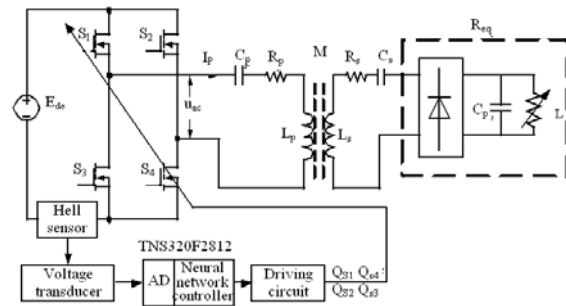
The diagram of generalized three-layer BP neural network is shown in Fig. 6. The input layer contains n neurons, hidden layer p neurons, output layer q neurons. Figure 6 Generalized three-layer BP neural network, $x_1 \sim x_n$: input vector of the neural network, $y_1 \sim y_q$: Output vector.

The input vector of the neural network is $X = [x_1, x_2, \dots, x_p, \dots, x_n]$, output vector $Y = [y_1, \dots, y_m, \dots, y_q]$. The excitation function from hidden layer to output layer is important to influence the network performance.

For the controller, mean square error is selected as performance index which characterizes the performance of the neural network controller.

According to the system control configuration, the SS-type voltage-fed ICPT system based on BP neural network control is built. Its diagram is shown in Fig. 7.

The input current is regarded as the input of the controller to control the input power of the ICPT system. The input current is detected to be voltage signal by hall sensor. The voltage signal is turned into standard signal for AD of DSP. In order to process discrete signal, the neural network must be discretized for the system neural network controller. The error operation, the neural network control, the system frequency transformation are accomplished by DSP (TMS320F2812). The square wave can't drive the switching devices directly. So, an extra driving circuit is necessary.


 Fig. 6: Generalized three-layer BP neural network, $x_1 \sim x_n$: input vector of the neural network, $y_1 \sim y_q$: output vector

 Fig. 7: Structures of ICPT system with neural network control, hall sensor: AC transformer, TMS320F2812: The controller, (Q_{s1}, Q_{s4}) : Drive of S_1 and S_4 , (Q_{s2}, Q_{s3}) : Drive of S_2 and S_3

EXPERIMENT RESULTS

In order to validate the feasibility of control approach, the circuit of SS-type voltage-fed ICPT system is built, the parameters are shown in Table 1. The proposed method will be compared with PID control method.

The experimental result in load perturbation is shown in Fig. 8.

From Fig. 8 it can be known that the dynamic response process just takes 5 m sec (less than 13 msec of PID) to successfully achieve tracking the reference value when the load resistance changes from 20-50 Ω . Concluding the PID control results as shown in Fig. 8b it is obvious that PID control method produces a greater disturbance which reaches 2A with respect to the proposed method. Therefore, this PID control method will be not suitable to the input power control. From this measured waveform it is evident that the input power is controlled by the proposed method when the load resistance surges.

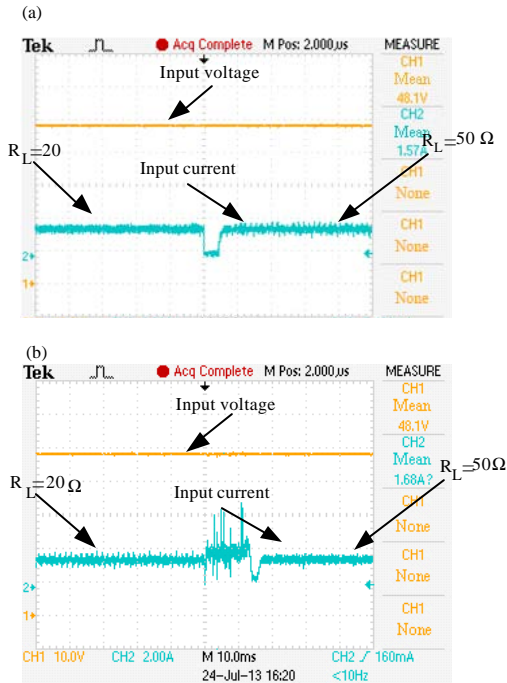


Fig. 8(a-b): Contrast experimental result based on BP neural network and PID in load perturbation, input voltage: Constant, input current: When resistor is changed it adjusts

Table 1: Parameters of experimental system

| Parameters | Values |
|--|--------------|
| DC input supply (V_{dc}) | 48V |
| Primary resonant inductance (L_p) | 559 μ H |
| Primary resonant capacitance (C_p) | 0.14 μ F |
| Secondary resonant capacitance (L_s) | 524 μ H |
| Secondary resonant inductance (C_s) | 0.14 μ F |
| Mutual inductance (M) | 492 μ H |

CONCLUSION

Due to the phenomenon that the input power is inconsistent with the load power demand in the voltage-fed inductively coupled power transfer system, so it is essential to control the input power. It is found that the input power is affected by system operating frequency, load resistance, input voltage. The input power presents a nonlinear negative correlation relationship with system operating frequency. The input power is controlled without overshoot by the designed controller. By introducing this control approach, the problem of input power control can be satisfactorily resolved.

ACKNOWLEDGMENTS

This research work is financially supported by National High-tech R and D Program of China

(863 Program) (No. 2013AA092401). I also would like to give my special thanks to the reviewers of this study for their contributions to this work. We are very grateful to all reviewers for their constructive comments on this study.

REFERENCES

- Boys, J.T., G.A. Covic and Y. Xu, 2003. DC analysis technique for inductive power transfer pick-ups. IEEE Power Elect. Lett., 1: 51-53.
- Hu, A.P., 2001. Resonant converter for IPT power supplies. Ph.D. Thesis, Department of Electrical and Electronic Engineering, University of Auckland, New Zealand.
- Li, Y.L., Y. Sun and X. Dai, 2012. Controller design for an uncertain contactless power transfer system. Inform. Technol. J., 11: 971-979.
- Li, Y.L., Y. Sun and X. Dai, 2013. i-Synthesis for frequency uncertainty of the ICPT system. IEEE Trans. Ind. Electron., 60: 291-300.
- Si, P., A.P. Hu, S. Malpas and D. Budgett, 2008. A frequency control method for regulating wireless power to implantable devices. IEEE Trans. Biomed. Circuits Syst., 2: 22-29.
- Sun, Y., X. Lv, Z. Wang and C. Tang, 2012. A quasi sliding mode output control for inductively coupled power transfer system. Inform. Technol. J., 11: 1744-1750.
- Tang, C.S., Y. Sun, Y.G. Su, S.K. Nguang and A.P. Hu, 2009. Determining multiple Steady-state ZCS operating points of a Switch-mode contactless power transfer system. IEEE Trans. Power Electron., 24: 416-425.
- Tian, Y., Y. Sun, Y. Su, Z. Wang and C. Tang, 2012. Neural network-based constant current control of dynamic wireless power supply system for electric vehicles. Inform. Technol. J., 11: 876-883.
- Wang, C.S., G.A. Covic and O.H. Stielau, 2004. Power transfer capability and bifurcation phenomena of loosely coupled inductive power transfer systems. IEEE Trans. Ind. Electron., 51: 148-157.
- Wang, Z.H., X. Lv, Y. Sun, X. Dai and Y.P. Li, 2012. A simple approach for load identification in current-fed inductive power transfer system. Proceedings of the International Conference on Power System Technology, October 30-November 2, 2012, Auckland, pp: 1-5.
- Wang, Z.H., Y.P. Li, Y. Sun, C.S. Tang and X. Dai, 2013a. An efficiency optimization strategy with segmented optimal frequency in the common inductive power transfer platform. Inform. Technol. J., 12: 1512-1521.

- Wang, Z.H., Y.P. Li, Y. Sun, C.S. Tang and X. Lv, 2013b. Load detection model of voltage-fed inductive power transfer system. *IEEE Trans. Power Electron.*, 28: 5233-5243.
- Wu, H.H., G.A. Covic, J.T. Boys and D.J. Robertson, 2011. A series-tuned inductive-power-transfer pickup with a controllable AC-voltage output. *IEEE Trans. Power Electron.*, 26: 98-109.
- Wu, Y., Y. Sun, Y. Tian, F. Yang and Y. Su, 2013. Study on voltage-stabilizing control of ICPT system. *Inform. Technol. J.*, 12: 664-671.
- Zhang, L., Y. Sun, Z. Wang and C. Tang, 2013. Analysis of bifurcation phenomena of voltage-fed inductively coupled power transfer system varying with coupling coefficient. *Inform. Technol. J.*, 12: 1176-1183.